Spectroscopic Characterization of the Heme-Binding Sites in *Plasmodium falciparum* Histidine-Rich Protein 2[†]

Clara Y. H. Choi,[‡] Jose F. Cerda,[§] Hsiu-An Chu,[§] Gerald T. Babcock,[§] and Michael A. Marletta*[,‡]

Department of Biological Chemistry, Division of Medicinal Chemistry, and the Howard Hughes Medical Institute, University of Michigan, Ann Arbor, Michigan 48109-0606, and Department of Chemistry and LASER Laboratory, Michigan State University, East Lansing, Michigan 48824-13220

Received July 20, 1999; Revised Manuscript Received October 6, 1999

ABSTRACT: Proteolysis of hemoglobin provides an essential nutrient source for the malaria parasite *Plasmodium falciparum* during the intraerythrocytic stage of the parasite's lifecycle. Detoxification of the liberated heme occurs through a unique heme polymerization pathway, leading to the formation of hemozoin. Heme polymerization has been demonstrated in the presence of *P. falciparum* histidine-rich protein 2 (PfHRP2) [Sullivan, D. J., Gluzman, I. Y., and Goldberg, D. E. (1996) *Science* 271, 219−221]; however, the molecular role that PfHRP2 plays in this polymerization is currently unknown. PfHRP2 is a 30 kDa protein composed of several His-His-Ala-His-His-Ala-Ala-Asp repeats and is present in the parasite food vacuole, the site of hemoglobin degradation and heme polymerization. We found that, at pH 7.0, PfHRP2 forms a saturable complex with heme, with a PfHRP2 to heme stoichiometry of 1:50. Spectroscopic characterization of heme binding by electronic absorption, resonance Raman, and EPR has shown that bound hemes share remarkably similar heme environments as >95% of all bound hemes are six-coordinate, low-spin, and bis-histidyl ligated. The PfHRP2−ferric heme complex at pH 5.5 (pH of the food vacuole) has the same heme spin state and coordination as observed at pH 7.0; however, polymerization occurs as heme saturation is approached. Therefore, formation of a PfHRP2−heme complex appears to be a requisite step in the formation of hemozoin.

Malaria is a major cause of morbidity and mortality, responsible for 200 million infections and 1−3 million deaths annually (*1*). The causative agent of malaria is the protozoan parasite *Plasmodium*, of which *Plasmodium falciparum* is the most virulent. *P. falciparum* spends a portion of its life cycle inside human erythrocytes. During this intraerythrocytic stage, *P. falciparum* ingests 25−75% of the host cell hemoglobin (*2*). Hemoglobin is degraded inside the parasite's food vacuole (pH 4.5−5.5) by proteases (*3*), and the amino acids from the degraded globin are used as the building blocks for the parasite's own intermediary metabolism. Upon hemoglobin cleavage, free heme is released (*4*). Because free heme is cytotoxic, detoxification of the liberated heme is critical for the parasite's survival (*5*, *6*). In mammals, free heme is degraded by the heme oxygenase/biliverdin reductase pathway. In contrast, *P. falciparum* achieves heme detoxification by polymerizing free heme into an insoluble crystalline material called hemozoin (also termed malaria pigment). Hemozoin is believed to be structurally identical to β-hematin, in which the ferric iron of one heme is coordinated by the propionate carboxylate group of an adjacent heme (*7*, *8*). The mechanism of heme polymerization within *P. falciparum* is a question that has often been debated, and several hypotheses have been advanced over the years. Some have proposed that heme polymerization is a spontaneous process occurring in the acidic environment of the food vacuole (*9*, *10*). While heme polymerization can occur in the absence of any protein, the necessary reaction conditions are far from physiologic, requiring both high acetic acid concentration (6 M) and high temperature (70 °C) (*7*). Reports of β-hematin synthesis under more physiological conditions have been communicated (*10*); however, those results have subsequently been challenged (*11*). The observation made by Slater and Cerami that whole *Plasmodium* lysate can mediate hemozoin formation in vitro (*12*) added support to the hypothesis that heme polymerization requires some component of parasitic origin. Sullivan et al. demonstrated that *Plasmodium* histidine-rich protein 2 and 3 can mediate heme polymerization in vitro (*13*) and proposed that HRPs present inside the food vacuole are responsible for heme polymerization. More recently, Ziegler et al. reported that incubation of heme with peptide dendrimers containing the repetitive sequence of *P. falciparum* histidine-rich protein 2 produced β-hematin (*14*).

P. falciparum histidine-rich protein 2 (PfHRP2)[1] is a 30 kDa protein with histidine and alanine residues constituting 76% of the entire protein. The highly repetitive amino acid sequence of PfHRP2 is comprised of several repeating sequences of His-His-Ala-His-His-Ala-Ala-Asp (*15*, *16*). While both catalytic as well as scaffolding roles have been

[†] This research has been supported by HHMI (M.A.M.) and by NIH GM25480 (G.T.B.). Clara Y. H. Choi is a trainee in the Medical Scientist Training Program at the University of Michigan funded by Grant T32 GM 07863.

* To whom correspondence should be addressed. Department of Biological Chemistry, University of Michigan Medical School, Ann Arbor, MI 48109-0606.

[‡] Department of Biological Chemistry, University of Michigan.

[§] Michigan State University.

10.1021/bi991665k CCC: $18.00
Published on Web 12/04/1999

proposed for HRPs (*13*), the exact molecular role that this highly unusual protein plays in hemozoin formation is unknown. However, the fact that heme polymerization is both unique to the parasite and vital to their survival makes this an ideal drug target. In order for PfHRP2 to mediate heme polymerization, it is likely that PfHRP2 interacts with heme; however, the basis for that interaction has not been explored. Here, we show that PfHRP2 binds multiple heme molecules. Furthermore, using electronic absorption, resonance Raman, and EPR spectroscopies, we show that each of the bound heme molecules in the PfHRP2−heme complex is coordinated by two protein histidines.

MATERIALS AND METHODS

Materials. The PfHRP2 overexpression plasmid was a gift of Dr. Daniel Goldberg (Washington University, St. Louis, MO). *Escherichia coli* BL21(DE3) competent cells and His-Bind Resin were purchased from Novagen. IPTG and ampicillin were from Boehringer Mannheim. Slide-A-Lyser dialysis membranes and the BCA Protein Assay Kit were from Pierce. Ultrafree spin concentrators were purchased from Millipore. $^{12}C^{16}O$ (99.5%) gas was from Matheson, and $^{13}C^{18}O$ (97%) gas was purchased from Isotech, Inc. (Miamisburg, OH). Quantitative amino acid analysis was done at the University of Michigan Biomedical Research Core Facility. All other chemicals were purchased from Sigma Chemical Co. unless otherwise stated.

Purification. PfHRP2 was expressed and purified as previously described (*13*) with the following modifications: Recombinant *E. coli* was grown in 2xYT media [16 g of casein enzymatic hydrolysate, 10 g of yeast extract (Difco), and 5 g of NaCl/1 L] with 100 μg/mL ampicillin. Cultures were grown at 37 °C until an OD_{600} of 0.6 was reached. The incubation temperature was then lowered to room temperature. After 30 min at room temperature, IPTG was added (final concentration of 0.5 mM). Cells were grown overnight at room temperature and harvested 12−16 h postinduction by centrifugation.

Protein concentrations were determined by the BCA protein concentration assay using BSA as the standard. Quantitative amino acid analysis indicated that no correction factor was needed for the BCA assay.

Sample Preparation. A stock heme solution was made by dissolving hemin chloride in 0.1 M NaOH, and the concentration of the heme solution was determined spectroscopically (ϵ_{385}= 58.44 mM^{-1} cm^{-1}) (*17*).

The time required for complete heme binding by PfHRP2 was determined as follows. For the pH 7.0 sample, electronic absorption spectra were recorded every 5 min after heme was added to PfHRP2. Heme binding to PfHRP2 was complete within 5 min as there were no changes in the PfHRP2−heme spectra after this time. When PfHRP2 and heme were mixed in 100 mM Mes (pH 5.5), electronic absorption spectra were recorded every 30 min. At pH 5.5, the Soret absorbance increased with time until it reached a plateau at 2−2.5 h; hence, the minimum time required for heme binding at pH 5.5 was determined to be 2−2.5 h.

The PfHRP2−ferric heme complex (at pH 7.0 or 9.0) was generated by mixing a 1:50 molar ratio of PfHRP2:heme in 100 mM Hepes (pH 7.0) or 100 mM Taps (pH 9.0). This mixture was incubated at room temperature for 5 min to allow complete heme binding.

The PfHRP2−ferric heme complex at pH 5.5 was made by incubating PfHRP2 and heme in 100 mM Mes (pH 5.5) at 37 °C for 2−15 h. All spectroscopic studies of the PfHRP2−heme complex at pH 5.5 were done using samples with a PfHRP2:heme molar ratio of 1:10−1:30. The PfHRP2:heme ratio was kept below 1:50 because, at pH 5.5, PfHRP2:heme ratio greater than 1:50 led to initiation of heme polymerization and precipitation of the product.

The sample of the PfHRP2−ferric heme complex was deoxygenated in a cuvette equipped with a rubber septum with 10 vacuum/argon cycles with a 2 min equilibration period between each cycle. A saturated sodium dithionite solution was made in a 3 mL, Teflon-sealed, argon-filled vial by adding deoxygenated water to sodium dithionite. Using a gas-tight syringe (Hamilton), 2−5 μL of the saturated dithionite solution was added to the PfHRP2−ferric heme sample to generate the PfHRP2−ferrous heme complex. The PfHRP2−ferrous heme−CO complex was obtained by placing the PfHRP2−ferrous heme complex under CO (1 atm) for 5 min.

Electronic Absorption Spectroscopy. All electronic absorption spectra were recorded on a Cary 3E spectrophotometer. Buffer conditions and PfHRP2/heme concentrations are described in the figure legends. All spectra were recorded at room temperature unless otherwise specified.

Determination of the Number of Heme-Binding Sites. Spectroscopic Heme Titration. The number of heme-binding sites was determined using the methods described by Tsutsui and Mueller (*18*) with slight modifications. A stock solution of 1 mM heme was made in 0.1 M NaOH. This heme solution was simultaneously titrated into two cuvettes, one containing 0.2 μM PfHRP2 in 100 mM Hepes (pH 7.0) and the other, the reference cuvette, containing buffer. Temperature was set at 37 °C using a Neslab RTE-100 temperature controller. Heme was added, in 1 μM increments, and difference absorption spectra were recorded after each addition. The difference spectra had a maximum at 416 nm and a minimum at 368 nm. The heme binding curve was constructed by plotting ΔA_{416} versus the heme concentration. The heme-binding curve was fitted to the following equilibrium binding equation (*19*):

$$RL^* = [(L_t^* + R_t + K_d) - [(L_t^* + R_t + K_d)^2 - 4R_tL_t^*]^{1/2}]/2 \quad (1)$$

where L^* = free ligand concentration; R_t = total receptor concentration; L_t^* = total ligand concentration.

Determination of the Number of Heme-Binding Sites. HPLC Quantitation. One hundred molar excess of heme was added to PfHRP2 in 100 mM Hepes, pH 7.0. This mixture was loaded on a Pharmacia PD-10 desalting column to

[1] Abbreviations: PfHRP2, *Plasmodium falciparum* histidine-rich protein 2; kDa, kilodalton(s); IPTG, isopropyl-β-D-thiogalactopyranoside; BSA, bovine serum albumin; BCA, bicinchoninic acid; CO, carbon monoxide; Hepes, 4-(2-hydroxyethyl)-1-piperazineethanesulfonic acid; Taps, *N*-tris(hydroxymethyl)methyl-3-aminopropanesulfonic acid; Mes, 2-(*N*-morpholino)ethanesulfonic acid; NaOH, sodium hydroxide; HPLC, high-performance liquid chromatography; RR, resonance Raman; EPR, electron paramagnetic resonance; Hb, hemoglobin; Mb, myoglobin; sGC, soluble guanylate cyclase; TFA, trifluoroacetic acid; PPIX, protoporphyrin IX; Im, imidazole; PP, protoporphyrin IX; *N*-MeIm, *N*-methyl imidazole; Cyt b_{559}, cytochrome b_{559}; SD, standard deviation.

remove excess heme. Those fractions containing the PfHRP2−heme complex were collected, and their heme concentrations determined using the HPLC method modified from that described by Brandish et al. (*20*). Myoglobin was used as the heme standard.

Horse heart myoglobin (5 mg/mL) was prepared in 100 mM potassium phosphate (pH 7.4). This stock solution was diluted 1:80 in phosphate buffer, placed in a quartz cuvette, sealed with a rubber septum, deoxygenated (as described under *Sample Preparation* in this section), and reduced with saturated solution of sodium dithionite. The heme concentration was determined spectroscopically ($\epsilon = 121\ mM^{-1}\ cm^{-1}$) (*21*). The myoglobin stock was diluted 1−10 μM in heme in order to generate a standard curve. Myoglobin standards and the PfHRP2−ferric heme samples were analyzed for heme content using the Beckman HPLC equipped with a 126NMP pump, 168 photodiode array detector, and 508 autosampler. Each sample (25 μL) was injected into a Protein C4 (0.2 μm, 25 cm × 2.1 mm) column (Vydac) that was preequilibrated with 0.1% aqueous trifluoroacetic acid (TFA) (Pierce) at 0.2 mL/min. The column was developed with a linear gradient of 0.1% aqueous TFA to 0.1% TFA in 75% acetonitrile over 4 mL, followed by a linear gradient of 0.1% TFA in 75% acetonitrile to 0.1% TFA in 100% acetonitrile over 0.6 mL. Finally, 0.1% TFA in 100% acetonitrile was applied to the column (over 0.4 mL). Heme was detected at 400 nm. A standard curve was constructed by plotting myoglobin heme concentration versus peak area, and this standard curve was used to calculate the heme concentration in the PfHRP2−heme sample.The concentration of PfHRP2 was determined using the BCA-enhanced assay as described in the Pierce BCA protein assay kit. Heme was found to interfere with the BCA assay; hence, PfHRP2 concentration was determined in the absence of heme. The same concentration of PfHRP2 in 100 mM Hepes, pH 7.0, was loaded on a PD-10 column and eluted with Hepes as before. The same fractions as those used to determine the heme concentration were collected, and BCA-enhanced assay was used to determine the protein concentration. New PD-10 columns were used for each run to minimize experiment to experiment variability. PfHRP2 concentration determined this way was found to vary by 1.8% between runs. The PfHRP2:heme stoichiometry was calculated by dividing the heme concentration (as determined by the HPLC method) by the protein concentration (as determined using the BCA enhanced assay).

Resonance Raman Spectroscopy. The resonance Raman spectra of the PfHRP2−ferric heme complex and the PfHRP2−ferrous heme−CO complex were collected with 413.1 nm excitation light from a Kr^+ laser (Coherent K-90). The spectra of the PfHRP2−ferrous heme complex were collected with 424 nm excitation produced by a stilbene dye laser (Coherent CR599) which was pumped by an argon laser (Coherent Innova 200). The laser power was kept at 10 mW. The resonance Raman scattering was focused onto a spectrometer (Spex 1877 Triplemate) and detected with a liquid nitrogen cooled CCD detector (EG&G OMA 4, model 1530-CUV-1024S). Calibration was done using toluene, and the spectra were averaged for 15−30 min. All spectra were collected using a spinning cell that was sealed with a septum. The sample was maintained at 10 °C. The heme vibrational modes were assigned according to Callahan and Babcock (*22*) and Choi et al. (*23*, *24*)

The resonance Raman samples of the PfHRP2−ferric heme complex were prepared with the following composition: (i) 0.8 μM PfHRP2 and 40 μM heme in 100 mM Hepes, pH 7.0; (ii) 4 μM PfHRP2 and 40 μM heme in 100 mM Mes, pH 5.5; (iii) 0.8 μM PfHRP2, and 40 μM heme in 100 mM Taps, pH 9.0.

Electron Paramagnetic Resonance Spectroscopy. EPR samples were prepared by incubating PfHRP2 (2 μM for the pH 7.0 and 9.0 samples or 5 μM for the pH 5.5 sample) with 100 μM heme overnight at 37 °C. After 16 h of incubation, the PfHRP2−ferric heme solutions were centrifuged (14000*g* for 5 min) to remove any precipitate. Each sample was further concentrated to approximately 150 μM in heme using Ultrafree-4 or Ultrafree-0.5 (10,000 MWNL) spin concentrators. Glycerol (20 vol %) was added to each sample. EPR spectra were obtained with a Bruker ESR300E instrument equipped with an Oxford ESR900 continuous-flow cryostat. The following conditions were used for all EPR measurements: microwave power, 6.30 mW; modulation amplitude, 20 G; time constant, 0.08 s; sweep time, 168 s; gain, 1.60×10^4; temperature, 10 K. To quantitate the concentration of high spin heme present in each sample, the method described by Babcock et al. (*25*) was used, using metmyoglobin (horse heart) fluoride as the standard. EPR conditions for metmyoglobin and the PfHRP2−ferric heme samples were as follows: frequency, 9.4 GHz; power, 12.6 mW; time constant, 0.041 s; modulation frequency, 100 kHz; modulation amplitude, 20 G; temperature, 10 K; gain, 1.25×10^4 (PfHRP2−heme) or 1.6×10^3 (metmyoglobin). These samples were normalized to gain of 1.6×10^3. The total heme concentration in each of the EPR samples was determined using the HPLC heme quantitation method described above.

RESULTS

Electronic Absorption Spectroscopy. The electronic absorption spectrum of the PfHRP2−ferric heme complex has a single Soret peak centered at 414 nm; the α/β bands occur at 565 and 535 nm, respectively (Figure 1). Addition of dithionite reduces the heme and shifts the Soret peak to 427 nm, with sharply split α and β bands at 560 and 530 nm, respectively. Placing the PfHRP2−ferrous heme complex under 1 atm of CO shifts the Soret to 423 nm with α and β bands at 565 and 541 nm, respectively. The electronic absorption spectra of the three species are shown in Figure 1, and the peak positions are summarized in Table 1.

The environment of the *P. falciparum* food vacuole is acidic (pH 4.5−5.5); hence, heme binding by PfHRP2 was also studied at pH 5.5. Addition of heme to PfHRP2 in 100 mM Mes (pH 5.5) generated an electronic absorption spectrum identical to the pH 7.0 spectrum. As with the sample at pH 7.0, the Soret peak of the pH 5.5 sample was centered at 414 nm, with the α and β bands at 565 and 535 nm, respectively (Supporting Information). Addition of saturated sodium dithionite solution to a deoxygenated solution of PfHRP2−ferric heme caused the Soret peak to broaden, suggesting that, at pH 5.5, histidines of PfHRP2 do not coordinate ferrous heme. Bubbling CO gas through this solution resulted in appearance of the Soret peak centered at 423 nm within 5 min of adding CO. The overall shape of the PfHRP2−ferrous heme−CO complex (pH 5.5) optical spectrum is identical to that of the pH 7.0 sample (data not

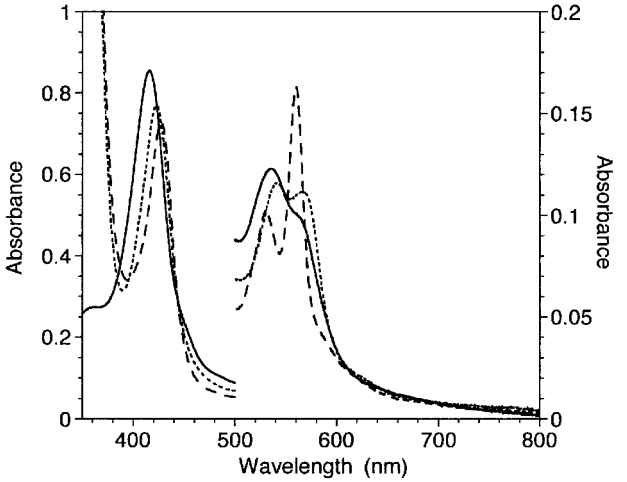

FIGURE 1: Electronic absorption spectra of the PfHRP2−ferric heme (−), -ferrous heme (- - -), and -ferrous heme−CO complexes (···). PfHRP2 (0.2 μM) was mixed with 10 μM heme in 100 mM Hepes, pH 7.0. After a 5 min incubation at room temperature, the electronic absorption spectrum of the PfHRP2−ferric heme complex was recorded. The PfHRP2−ferrous heme and PfHRP2−ferrous heme−CO complexes were prepared as described in the Materials and Methods. The left *y*-axis scale refers to the Soret region; the right *y*-axis scale refers to the α/β region.

Table 1: Electronic Absorption Spectra Peak Positions: PfHRP2−Ferric Heme, − Ferrous Heme, and Ferrous Heme−CO, Bis-imidazole Protoporphyrin Model compounds, Myoglobin−CO, and Soluble Guanylate Cyclase−CO

sample	Soret[e]	β[e]	α[e]
PfHRP2−ferric heme[a]	414	535	565
Fe^{3+} (PPIX) $(Im)_2Cl^-$ [b]	413	535	564
PfHRP2−ferrous heme[a]	427	530	560
Fe^{2+} (PPIX) $(Im)_2$[b]	426	530	559
PfHRP2−ferrous heme-CO[a]	423	541	565
Mb−CO[c]	424	540	579
sGC−CO[d]	423	541	567

[a] This work. [b] Babcock et al. (*27*). [c] Antonini et al. (*21*). [d] Stone et al. (*34*). [e] All wavelengths shown are in nanometers.

shown). This indicates that the iron-histidine bond is reestablished within 5 min of adding CO.

Determination of the Number of Heme-Binding Sites on PfHRP2. Spectrophotometric heme titration experiments were performed to determine the number of heme-binding sites on PfHRP2. Difference absorption spectra were recorded at varying heme concentrations and are shown in Figure 2a. A heme-binding curve, generated by plotting ΔA_{416} versus the heme concentration, is shown in Figure 2b. The linear portion of the binding curve represents complete binding of added heme, whereas the curved portion indicates the presence of unbound heme. Fitting this heme binding curve yielded a PfHRP2:heme binding stoichiometry of 51.76 $\pm$ 0.72 hemes/PfHRP2. The HPLC heme quantitation method was used as an independent measure of the number of heme-binding sites with the result of 47.3 $\pm$ 5.5 hemes/PfHRP2 ($n = 3$, mean $\pm$ SD).

Resonance Raman Spectroscopy. The resonance Raman spectra for the high- and low-frequency regions of the PfHRP2−ferric and −ferrous heme complexes are shown in Figure 3. The principal vibrational frequencies of the PfHRP2−ferric and −ferrous heme complexes are summarized in Table 2, along with the vibrational frequencies of bis-(imidazole) hemin model compounds.

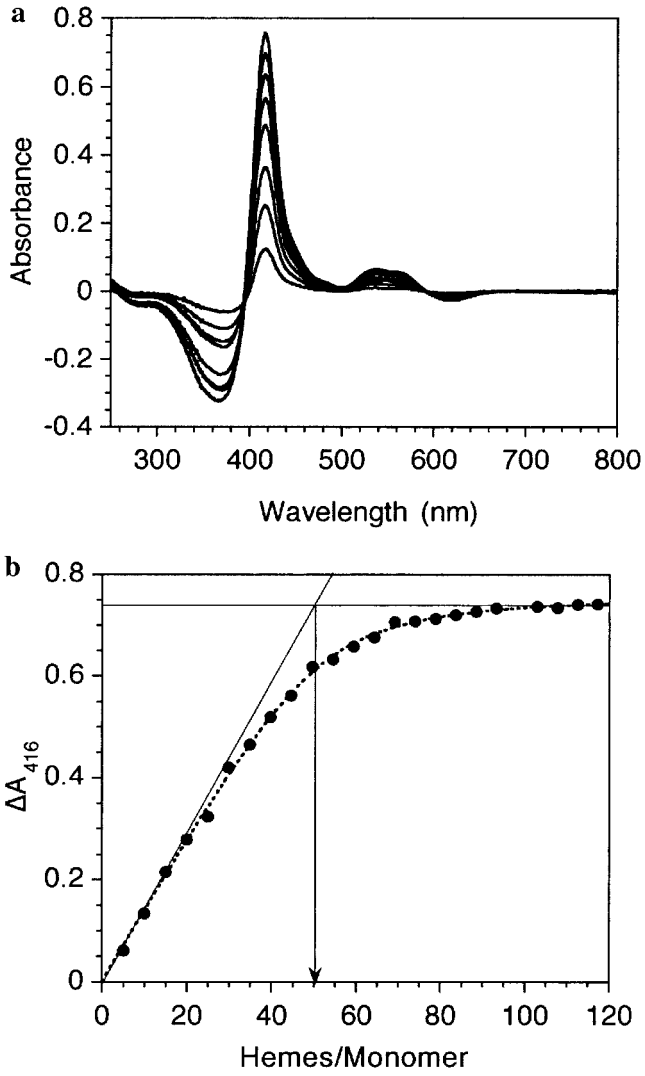

FIGURE 2: Determination of the number of heme binding sites on PfHPR2. (a) Difference absorption spectra recorded from the heme titration experiment. A hemin solution (1 mM solution dissolved in 0.1 M NaOH) was simultaneously titrated into (i) a solution of 0.2 μM PfHRP2 in 100 mM Hepes, pH 7.0 and (ii) a reference cuvette containing Hepes buffer only. Hemin was titrated in 1 μM increments, and the temperature was maintained at 37 °C. Difference absorption spectra were recorded after each addition of heme. (b) A heme-binding curve generated from the difference absorption spectra by plotting ΔA_{416} vs the heme concentration. Equation 1 was used to fit the curve (···). The two straight lines (−) represent (i) the initial slope of the binding curve and (ii) complete binding of heme (i.e., ΔA maximum). A line drawn from the intersection of the first two lines to the abscissa (→) marks the saturation point of the heme-binding sites.

PfHRP2−Ferric Heme. The oxidation state marker, ν_4, appears at 1375 cm^{-1} as expected, indicating that heme is ferric. The ν_{10}, ν_3, and ν_2 bands are sensitive to the core size of the heme macromolecule and serve as the spin and coordination state markers. In the PfHRP2−ferric heme complex, the ν_{10}, ν_3, and ν_2 bands are located at 1640, 1505, and 1580 cm^{-1}, respectively, indicative of a six-coordinate, low-spin heme. Furthermore, the principal vibrational frequencies of the PfHRP2−ferric heme complex are very similar to those of bis-(imidazole) ferric protoporphyrin (Table 2) in which the heme is ligated by two imidazoles. The PfHRP2−ferric heme samples at pH 5.5 and 9.0 yielded identical resonance Raman spectra to those at pH 7.0 (Supporting Information).

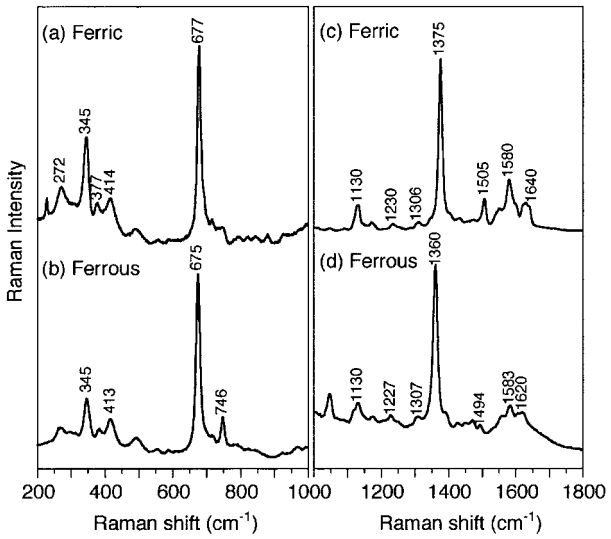

FIGURE 3: Low- and high-frequency regions of the resonance Raman spectra of the ferric heme− and ferrous heme−PfHRP2 complexes (0.8 μM PfHRP2 and 40 μM heme in 100 mM Hepes, pH 7.0): The resonance Raman spectra of the PfHRP2−ferric heme complex were obtained with 413.1 nm excitation (a and c). The resonance Raman spectra of the reduced, PfHRP2−ferrous heme complex were obtained with 424 nm excitation (b and d).

Table 2: Resonance Raman Frequencies and Mode Assignments: PfHRP2−Heme and Bis-imidazole Heme Model Compounds

mode	PfHRP2−Fe^{3+} heme[a]	$(Im)_2$ Fe^{3+} PP[b,c]	PfHRP2−Fe^{2+} heme[a]	$(Im)_2$ Fe^{2+} PP[b,c]
ν_{cc}	1620	1620	1620	1620
ν_{10}	1640	1640		1617
ν_{37}	1601	1602	1601	1604
ν_2	1580	1579	1584, 1563	1584
ν_3	1505	1502	1494, 1470	1493
ν_4	1375	1373	1360	1353
ν_{19}		1586		1583
ν_{11}		1562		1539
ν_{38}	1552	1554	1558	1560
ν_{28}	1468	1469	1470	1469
$\delta_s(=CH_2)$ (1)	1431	1435	1426	1431
ν_{29}		1402		1390
ν_{20}		1399		1392
$\delta_s(=CH_2)$ (2)	1346	1346		1337
ν_{21}		1306	1307	1306
$\nu_5+\nu_9$		1260		1254
ν_{13}		1230	1227	1225
$\nu_6+\nu_8$	1130	1130	1130	1130
ν_9	271	272		
ν_8	345	345	345	345
ν_7	677	677	675	675

[a] This work. [b] Choi et al. (*23*). [c] Choi et al. (*24*).

PfHRP2−Ferrous Heme. Addition of dithionite reduces the heme to generate the PfHRP2−ferrous heme complex. Reduction is complete as evidenced by the absence of the ferric oxidation state peak at 1375 cm^{-1}. The reduced PfHRP2−heme complex at pH 7.0 has ν_4, ν_3, and ν_2 bands at 1360, 1494, and 1583 cm^{-1}, respectively, characteristic of a six-coordinate, low-spin ferrous heme (Figure 3). Similarly, the pH 9.0 sample spectrum has the ν_4, ν_3, and ν_2 bands at the same position as the pH 7.0 sample (data not shown). Unlike the pH 9.0 sample, however, polarized resonance Raman spectra of the PfHRP2−ferrous complex at pH 7.0 reveals a very small population of high-spin ferrous heme, with the ν_3 and ν_2 bands appearing at 1470 and 1563 cm^{-1}, respectively (data not shown). Using resonance Raman spectroscopy, we are unable to quantitate the amount of heme that is high-spin.

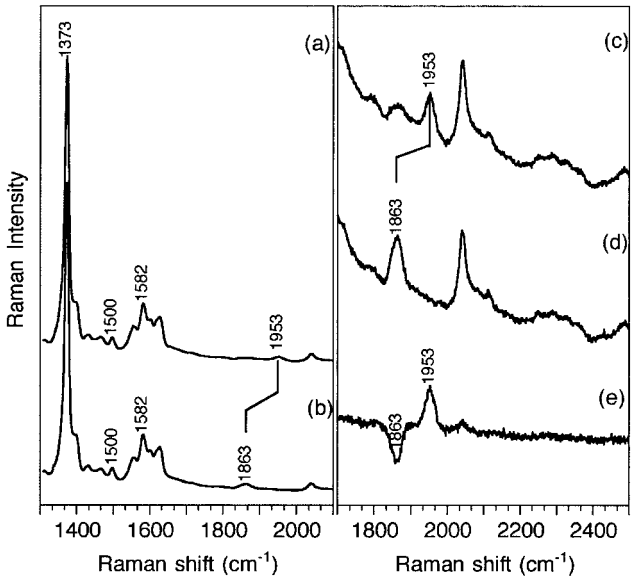

FIGURE 4: High-frequency region of the resonance Raman spectra of the PfHR2−ferrous heme−CO complex (0.8 μM PfHRP2 and 40 μM heme in 100 mM Hepes, pH 7.0) obtained with 413.1 nm excitation. (a and c) PfHRP2−ferrous heme−$^{12}C^{16}O$; (b and d) PfHRP2−ferrous heme-$^{13}C^{18}O$; (e) difference spectrum of $^{12}C^{16}O$ minus $^{13}C^{18}O$.

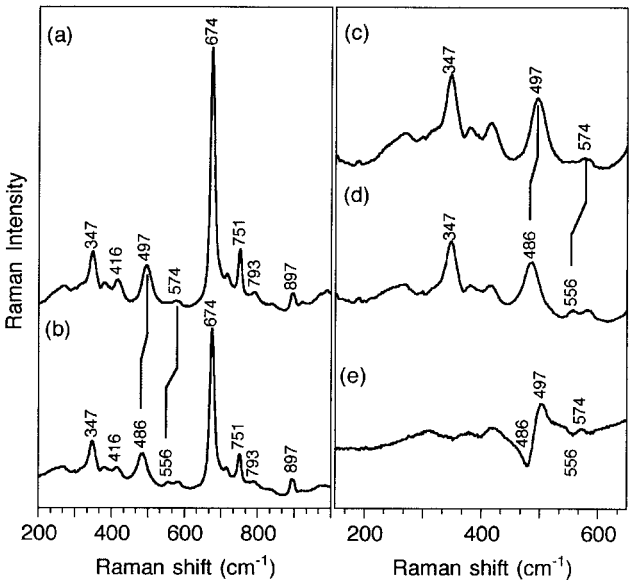

FIGURE 5: Low-frequency region of the resonance Raman spectra of the PfHRP2−ferrous heme−CO complex (0.8 μM PfHRP2 and 40 μM heme in 100 mM Hepes, pH 7.0) obtained with 413.1 nm excitation. (a and c) PfHRP2−ferrous heme−$^{12}C^{16}O$; (b and d) PfHRP2−ferrous heme−$^{13}C^{18}O$; (e) difference spectrum of $^{12}C^{16}O$ minus $^{13}C^{18}O$.

PfHRP2−Ferrous Heme−CO. The resonance Raman spectra of the high- and low-frequency regions of the PfHRP2−ferrous heme−CO complex are shown in Figures 4 and 5, respectively. The absence of a shoulder on the low-frequency side of ν_4 indicates that no photolysis of CO occurred under the experimental conditions that were used. The ν_2, ν_3, and ν_4 bands, located at 1582, 1500, and 1373 cm^{-1}, respectively, are characteristic of a CO-bound, six-coordinate heme. These values are similar to those of hemoglobin−CO (HbA-CO), myoglobin−CO (Mb-CO), and

Table 3: Resonance Raman Frequencies and Mode Assignments: Carbonmonoxy Complexes of PfHRP2−Ferrous Heme, Hemoglobin, Myoglobin, and Soluble Guanylate Cyclase

sample	PfHRP2−heme−$^{12}C^{16}O$[a]	PfHRP2−heme−$^{13}C^{18}O$[a]	HbA−CO[b]	Mb−CO[b,c]	sGC−CO[d]
ν_{cc}	n.o.[e]	n.o.	1622	1622	n.o.
ν_{10}	n.o.	n.o.	1633	1637	1629
ν_2	1582	1582	1586	1587	1581
ν_3	1500	1500	1500	1498	1500
ν_4	1373	1373	1372	1372	1371
ν(Fe−CO)	497	486	507	512	472
δ(Fe−C−O)	574	556	578	577	562
ν(C−O)	1953	1863	1951	1944	1987

[a] This work. [b] Tsubaki et al. (*35*). [c] Rimai et al. (*36*). [d] Deinum et al. (*37*). [e] n.o., not obtained.

soluble guanylate cyclase−CO (sGC-CO), three hemoprotein−CO adducts in which the hemes are coordinated by a histidine on one side and a CO molecule on the other (Table 3).

In the high-frequency region, there is one isotope-sensitive band. The peak at 1953 cm^{-1}, which we assign as the C−O stretching vibration [ν(C−O)], shifts to 1863 cm^{-1}, when the heavier $^{13}C^{18}O$ isotope is used (Figure 4, panels c and d). There are two isotope-sensitive bands in the low-frequency resonance Raman spectra (Figure 5). We assign the 497 and 574 cm^{-1} bands as the Fe−CO stretching frequency [ν(Fe−CO)] and the Fe−C−O bending mode [δ-(Fe−C−O)], respectively. These assignments were confirmed by isotope substitution with $^{13}C^{18}O$. In the presence of $^{13}C^{18}O$, the two bands shift to 489 and 556 cm^{-1}, respectively. The resonance Raman spectra of the PfHRP2−ferrous heme−CO complex are nearly identical at pH 5.5, 7.0, and 9.0 (Supporting Information), indicating that the heme environment is unaltered within the pH range explored.

EPR Spectroscopy. To further characterize the heme binding environment, EPR spectra of the PfHRP2−ferric heme complex were obtained. The major component represented in the EPR spectrum is low-spin, ferric heme, with *g*-values of 2.94, 2.26, and 1.62 (Figure 6). These *g*-values are characteristic of bis-imidazole ligated heme (*26*). The spectrum is significantly distorted, however, relative to those of other bis-imidazole, low-spin hemes (*27*), most likely reflecting magnetic interactions between the hemes bound to PfHRP2. EPR spectra of the PfHRP2−ferric heme samples at pH 5.5 and 9.0 were also collected, and both spectra gave identical *g*-values and similar line shapes as those for the pH 7.0 sample (Supporting Information).

There is a small population of high-spin heme as indicated by the $g = 6$ signal (Figure 6). The concentration of high-spin heme was quantified using ferrimyoglobin as the standard. High-spin heme concentrations of the PfHRP2−heme complex for four independent EPR samples were 1.6, 2.0, 2.2, and 7.4% of the total heme content.

Table 4 summarizes the *g*-values and the ligand field parameters [tetragonality (V/λ) and rhombicity ($|V/\lambda|$)] for the PfHRP2−ferric heme complex. Comparison of the ligand field parameters indicates that the tetragonality and rhombicity parameters of the PfHRP2−ferric heme complex closely resemble those hemes with two axial imidazole ligands [e.g., bis-(*N*-methylimidazole) ferric protoporphyrin IX (at neutral pH), maize cytochrome b_{559}, and spinach cytochrome b_{559}]. The ligand field parameters for bis-(*N*-methylimidazole) ferric protoporphyrin IX (at alkaline pH), which contains an imidazolate ligand (*27*) (Table 2), are distinctly different than those for the PfHRP2−ferric heme complex.

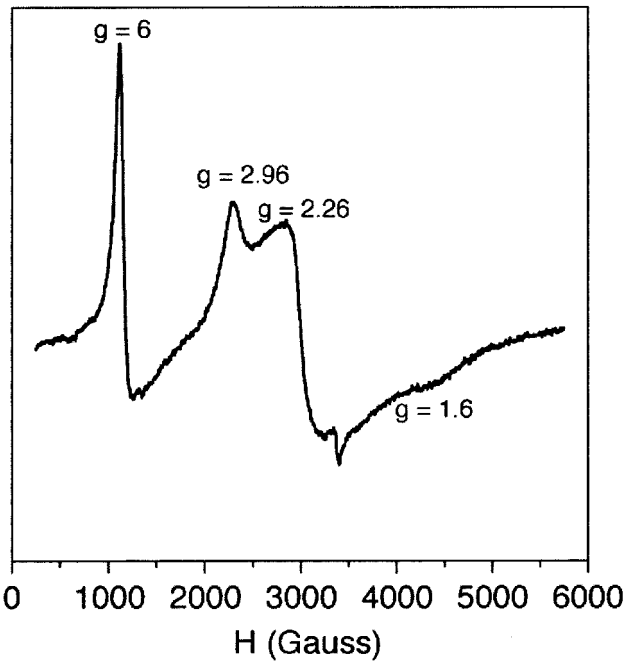

FIGURE 6: EPR spectrum of the PfHRP2−ferric heme complex in 100 mM Hepes, pH 7.0. EPR sample preparation is described in the Materials and Methods. EPR conditions were as follows: temperature, 10 K; frequency, 9.477 338 GHz, microwave power, 6.3 mW; gain, 1.6×10^4; modulation frequency, 100 kHz; modulation amplitude, 20.120 G; time constant, 81.92 ms; sweep field, 5500 G. The spectrum was obtained as the average of four scans.

Table 4: *g*-Values and Ligand Field Parameters: PfHRP2−ferric Heme and Various Low-Spin Ferric Heme Species

sample	g_z	g_y	g_x	tetragonality[c]	rhombicity[c]
PfHRP2−ferric heme[a]	2.94	2.26	1.62	2.02	0.52
Fe^{3+}PPIX (*N*-MeIm)$_2$ (neutral)[b]	2.95	2.26	1.52	1.87	0.56
Cyt b-559 (maize)[b]	2.94	2.27	1.54	1.92	0.57
Cyt b-559 (spinach)[b]	2.93	2.26	1.55	1.94	0.56
Fe^{3+}PPIX (*N*-MeIm)$_2$ (alkaline)[b]	2.74	2.27	1.72	2.8	0.67

[a] This work. [b] Babcock et al. (*27*). [c] Taylor axis system (*38*).

DISCUSSION

Spectroscopic Characterization of the PfHRP2−Ferric Heme Complex. PfHRP2 has an extraordinary capacity for binding heme. While recombinant PfHRP2 contains no heme as isolated, the PfHRP2−heme complex can easily be

generated by adding heme to PfHRP2 in solution. Both spectrophotometric heme titration and HPLC heme quantitation have revealed that PfHRP2 can bind approximately 50 mol of heme/mol of protein (Figure 2). Even more remarkably, the bound hemes share very similar environments as indicated by the appearance of a single Soret peak in the optical spectrum as well as single spin and coordination state markers in the resonance Raman spectra. Lacking a crystal structure, the means by which PfHRP2 is able to accommodate so many heme macrocycles is uncertain. We propose that the repetitive nature of the PfHRP2 amino acid sequence and the predicted α-helical secondary structure allow the protein to provide such similar environments for all of the bound hemes. Moreover, the ability of PfHRP2 to bind multiple hemes in homogeneous environments may be the key to heme polymerization.

Inside the *P. falciparum* food vacuole, hemoglobin degradation releases ferrous heme which rapidly becomes oxidized to ferric. These ferric hemes subsequently polymerize to form hemozoin (*2*). Hence, it is the ferric species that is of the highest physiological interest. The electronic absorption, resonance Raman, and EPR spectroscopic data presented here demonstrate that almost all of the hemes in the PfHRP2−ferric heme complex are low-spin, six-coordinate, and bis-imidazole ligated. Comparison of the PfHRP2−ferric heme complex spectra with those of other six-coordinate, low-spin, bis-imidazole ligated hemes reveal remarkable similarities, thereby further supporting our conclusion regarding the heme environment: first, optical spectra very similar to that of the PfHRP2−ferric heme complex have been reported using bis-(*N*-methylimidazole) ferric protoporphyrin IX model compound and cytochrome b_5 (*27*); second, the principal Raman frequencies of the PfHRP2−ferric heme complex are in good agreement with the bis-imidazole ferric heme model compound, chloroplast cytochrome b_{559} (*27*), neutrophil cytochrome b_{558} (*28*), and barley hemoglobin (*29*); third, the EPR spectrum of the PfHRP2−ferric heme complex shares similar *g*-values and ligand field parameters as bis-(*N*-methylimidazole) ferric protoporphyrin IX (at neutral pH), maize cytochrome b_{559}, and spinach cytochrome b_{559} (*27*).

Heme polymerization requires an acidic environment. Accordingly, electronic absorption, resonance Raman, and EPR spectra of the PfHRP2−ferric heme complex were obtained at pH 5.5. Data presented here demonstrate that the heme environment and the ligand structure are identical under both pH conditions, as the PfHRP2−ferric heme complex at pH 5.5 and 7.0 exhibits identical electronic absorption, resonance Raman, and EPR spectra. This indicates that, under the pH conditions in which this protein−heme complex is presumed to be present physiologically (i.e., pH 5.5), the hemes of the PfHRP2−ferric heme complex are still six-coordinate, low-spin, and bis-histidyl ligated.

While both electronic absorption and resonance Raman spectra did not show any high-spin heme species, EPR spectra of the PfHRP2−ferric heme complex at both pH 7.0 and 5.5 reveal a small population of high-spin heme with *g*-value of 6. The fact that there is such a small amount of high-spin heme (1.6−7.4%) present in the PfHRP2−ferric heme sample accounts for the fact that they were not detected in the electronic absorption and resonance Raman spectra.

On the basis of their work with peptide dendrimers containing the repeat motif of PfHRP2, Ziegler et al. suggested that the PfHRP2/heme interaction is due to π-stacking and electrostatic interaction and not due to histidine ligation of the heme iron (*14*). While π-stacking and electrostatic interactions likely play a role in stabilizing the PfHRP2−ferric heme complex, spectroscopic data presented here clearly demonstrate that each heme molecule is coordinated by two histidine residues from PfHRP2. Therefore, we conclude that histidine ligation is a major contributor in heme binding to PfHRP2.

Spectroscopic Characterization of the PfHRP2−Ferrous Heme Complexes. While the ferric heme complex of PfHRP2 may be the physiologically significant species, spectroscopic study of the PfHRP2−ferrous heme and PfHRP2−ferrous heme−CO complexes provide additional information about the heme environment. Both the optical spectrum (Figure 1) and the resonance Raman spectra (Figure 3b and 3d) indicate that the bound hemes in the PfHRP2−ferrous heme complex (at pH 7.0) are six-coordinate, low-spin, and bis-histidyl ligated. The reduced PfHRP2−heme complex shares a nearly identical optical spectra with both bis-(*N*-methylimidazole) ferrous protoporphyrin IX (Table 1) and reduced cytochrome b_{559} (*27*) and similar resonance Raman spectra as the bis-imidzole ferrous heme model compound (Table 2). On the basis of these results, we conclude that the majority of the bound hemes in the PfHRP2−heme complex at pH 7.0 remain six-coordinate and low-spin in both ferric and ferrous oxidation states. Similarly, chloroplast cytochrome b_{559} (*27*), neutrophil cytochrome b_{558} (*28*), and barley hemoglobin (*29*) all contain hemes that remain six-coordinate and low-spin in both oxidation states.

Addition of CO to the PfHRP2−ferrous heme complex yields the PfHRP2−ferrous heme−CO complex whose electronic absorption and resonance Raman spectra are characteristic of a histidine-ligated, six-coordinate, CO-bound heme. Similar optical and resonance Raman spectra are exhibited by the carbonmonoxy complexes of other histidine-ligated hemoproteins, such as hemoglobin and myoglobin (*21*). The fact that CO can bind to the PfHRP2−ferrous heme complex, which consists of bis-histidyl ligated hemes, means that CO must displace one of the axial histidines. This is not unprecedented. Both barley hemoglobin (wild type) and H64V/V68H double mutant of myoglobin have bis-histidyl ligated hemes. Upon addition of CO to either of these proteins, one of the axial histidine ligands is displaced by CO to form the CO adduct (*30*, *31*).

The inverse correlation that exists between the Fe−CO stretching frequency and the C−O stretching frequency has been well-established (*32*). As the π-back-donation from the d_π orbital of the iron to the empty π^* orbital of CO increases, the Fe−C bond strength and, hence, ν(Fe−CO) increase. Concurrently, the C−O bond weakens proportionally, and ν(C−O) decreases. Figure 7 shows a plot of ν(Fe−CO) versus ν(C−O) for several CO-bound hemoproteins with histidyl ligation (*32*). As seen in Figure 7, the PfHRP2−heme−CO complex falls on this correlation line, adding further support to the conclusion that the hemes of the PfHRP2−heme complex are coordinated by histidines.

pH Effects. The PfHRP2−ferric heme complex at pH 5.5 and pH 7.0 yielded nearly identical electronic absorption, resonance Raman, and EPR spectra, indicating that the heme

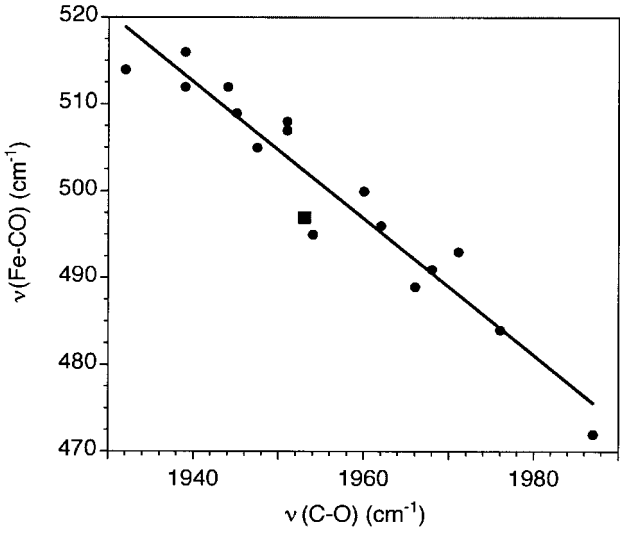

FIGURE 7: A plot of the Fe−CO stretching frequency versus the C−O stretching frequency. Carbonmonoxy complexes of metalloporphyrins and hemoproteins (●); the PfHRP2−ferrous heme−CO complex (■).

environment and the ligand structure of the PfHRP2−heme complex at pH 5.5 and 7.0 are very similar (i.e., majority of the bound hemes are bis-histidyl ligated at both pH 5.5 and 7.0). This suggests that the pK_a's of the PfHRP2 histidine residues are likely to be lower than that of free imidazole since PfHRP2 is able to provide unprotonated histidines to serve as heme ligands at pH 5.5. Furthermore, the remarkable similarities in the heme environments of the PfHRP2−ferric heme complex at pH 5.5 and 7.0 (as evidenced by spectroscopy) mean that we can use the pH 7.0 sample to study the heme-binding step independent of the polymerization step. Another advantage of studying the PfHRP2−ferric heme complex at pH 7.0 is that we are able to work with higher heme concentrations since heme solubility in aqueous solution increases as pH increases.

At pH 7.0, PfHRP2 binds ferric heme without any reactions taking place; hence, we are able to uncouple the binding step from the subsequent polymerization steps. Moreover, at pH 7.0, we can isolate and study the PfHRP2−ferric heme complex with all of the heme sites fully occupied. In contrast, the PfHRP2−ferric heme complex at pH 5.5 can only be studied if the PfHRP2:ferric heme ratio is maintained below 1:50. At pH 5.5, heme binding by PfHRP2 at a ratio greater than 1:50 leads to initiation of heme polymerization and precipitation of the product. Therefore, all of the spectroscopic data presented here with the pH 5.5 sample were performed using "subsaturating" ratio of PfHRP2:heme (i.e., PfHRP2:heme ratio of 1:10−1:30). Since most of the bound hemes are spectroscopically indistinguishable, whether the complex is fully or partially occupied with heme does not affect the spectra.

There are several possibilities as to why PfHRP2 can mediate heme polymerization at pH 5.5 and not at 7. One possibility is that the reaction is very slow or nonexistant at pH 7.0 simply because the polymerization is acid catalyzed. That is, a pH change could affect polymerization without altering heme binding to PfHRP2. Alternatively, there may be slight structural differences between the pH 5.5 and the pH 7.0 samples of the PfHRP2−heme complex that are not evident spectroscopically. For example, the histidines of PfHRP2 do not appear to coordinate ferrous heme at pH 5.5 while the PfHRP2−ferric heme and the PfHRP2−ferrous heme−CO complexes at pH 5.5 and 7.0 exhibit identical optical, resonance Raman, and EPR (for the ferric complex) spectra. The loss of ferrous heme binding at pH 5.5 may be due to subtle conformational differences between the pH 5.5 and the pH 7.0 complexes, and this may account for the lack of heme polymerizing activity at pH 7.0.

The fact that PfHRP2 does not coordinate ferrous heme at pH 5.5 is quite interesting and may be related to the recent findings of Monti et al. showing that ferrous protoporphyrin IX (i) does not polymerize and (ii) inhibits ferric protoporphyrin IX polymerization (*33*). Binding of ferrous protoporphyin IX by PfHRP2 would be unproductive since this would lead to the inhibition of polymerization. Therefore, there may be a teleologic reason for the fact that under heme polymerizing conditions (i.e., acidic environment), PfHRP2 appears to selectively bind ferric heme.

CONCLUSION

PfHRP2 can bind an unusually large number of hemes. There are approximately 50 available heme-binding sites per monomer of PfHRP2. There is a remarkable homogeneity in the heme environments such that the electronic absorption, resonance Raman, and EPR spectra of the PfHRP2−heme complex all indicate that greater than 95% of the hemes in the PfHRP2−heme complex are six-coordinate, low-spin, and bis-histidyl ligated. Since there are 98 histidine residues in PfHRP2, this result suggests that every histidine residue of PfHRP2 coordinates heme when all of the heme sites are occupied.

Not only is the heme polymerization process interesting chemically, it also has extremely important implications in antimalarial therapy. The uniqueness of the *Plasmodium* heme detoxification pathway makes for an exceedingly attractive drug target. Understanding the molecular mechanism of heme polymerization is the necessary first step to rational drug design. Having examined what may be the first step in the PfHRP2-mediated heme polymerization (i.e., binding of heme by PfHRP2), efforts to elucidate the subsequent steps are currently underway.

ACKNOWLEDGMENT

We thank Marilena diValentin (MSU) and the members of the Marletta lab for helpful discussion.

SUPPORTING INFORMATION AVAILABLE

Electronic absorption, resonance Raman, and EPR spectra of the PfHRP2−heme complex at pH 5.5. This material is available free of charge via the Internet at http://pubs.acs.org.

REFERENCES

1. Bradley, T. (1996) www-micro.msb.le.ac.uk/Bradley/Bradley.html.
2. Meshnick, S. R. (1996) *Ann. Trop. Med. Parsitol. 90*, 367−372.
3. Olliaro, P. L., and Goldberg, D. E. (1995) *Parasitol. Today 11*, 294−297.
4. Rosenthal, P. J., and Meshnick, S. R. (1996) *Mol. Biochem. Parasitol. 83*, 131−139.

5. Orjih, A. U., Banyal, H. S., Chevli, R., and Fitch, C. D. (1981) *Science 214*, 667−669.
6. Fitch, C. D., Chevli, R., Banyal, H. S., Phillips, G., Pfaller, M. A., and Krogstad, D. J. (1982) *Antimicrob. Agents Chemother. 21*, 819−822.
7. Slater, A. F. G., Swiggard, W. J., Orton, B. R., Flitter, W. D., Goldberg, D. E., Cerami, A., and Henderson, C. B. (1991) *Proc. Natl. Acad. Sci. U.S.A. 88*, 325−329.
8. Bohle, D. S., Dinnebier, R. E., Madsen, S. K., and Stephens, P. W. (1997) *J. Biol. Chem. 272*, 713−716.
9. Dorn, A., Stoffel, R., Matile, H., Bubendorf, A., and Ridley, R. G. (1995) *Nature 374*, 269−271.
10. Egan, T. J., Ross, D. C., and Adams, P. A. (1994) *FEBS Lett. 352*, 54−57.
11. Pandey, A. V., and Tekwani, B. L. (1996) *FEBS Lett. 393*, 189−192.
12. Slater, A. F. G., and Cerami, A. (1992) *Nature 355*, 167−169.
13. Sullivan, D. J., Gluzman, I. Y., and Goldberg, D. E. (1996) *Science 271*, 219−221.
14. Ziegler, J., Chang, R. T., and Wright, D. W. (1999) *J. Am. Chem. Soc. 121*, 2395−2400.
15. Wellems, T. E., and Howard, R. J. (1986) *Proc. Natl. Acad. Sci. U.S.A. 83*, 6065−6069.
16. Panton, L. J., McPhie, P., Maloy, W. L., Wellems, T. E., Taylor, D. W., and Howard, R. J. (1989) *Mol. Biochem. Parasitol. 35*, 149−160.
17. Dawson, R. M. C., Elliot, D. C., Elliot, W. H., and Jones, K. M. (1995) *Data for Biochemical Research*, Oxford University Press Inc., New York.
18. Tsutsui, K., and Mueller, G. C. (1982) *J. Biol. Chem. 257*, 3925−3931.
19. Hulme, E. C. (1992) *Receptor−Ligand Interactions: A Practical Approach*, Oxford University Press, New York.
20. Brandish, P. E., Buechler, W., and Marletta, M. A. (1998) *Biochemistry 37*, 16898−16907.
21. Antonini, E., and Brunori, M. (1971) *Hemoglobin and Myoglobin in Their Reactions with Ligands*, North-Holland Publishing Co., Amsterdam.
22. Callahan, P. M., and Babcock, G. T. (1981) *Biochemistry 20*, 952−958.
23. Choi, S., Spiro, T. G., Langry, K. C., Smith, K. M., Budd, D. L., and Mar, G. N. L. (1982) *J. Am. Chem. Soc. 104*, 4345−4351.
24. Choi, S., Lee, J. J., Wei, Y. H., and Spiro, T. G. (1983) *J. Am. Chem. Soc. 105*, 3692−3707.
25. Babcock, G. T., Vickery, L. E., and Palmer, G. (1978) *J. Biol. Chem. 253*, 2400−2411.
26. Blumberg, W. E., and Peisach, J. (1968) in *Probes of Structure and Function of Macromolecules and Membranes, Vol. II, Probes of Enzymes and Hemoproteins* (Chance, B., Yonetani, T., and Mildvan, A. S., Ed.) pp 215−228, Academic Press, New York.
27. Babcock, G. T., Widger, W. R., Cramer, W. A., Oertling, W. A., and Metz, J. G. (1985) *Biochemistry 24*, 3638−3645.
28. Hurst, J. K., Loehr, T. M., Curnutte, J. T., and Rosen, H. (1991) *J. Biol. Chem. 266*, 1627−1634.
29. Das, T. K., Lee, H. C., Duff, S. M. G., Hill, R. D., Peisach, J., Rousseau, D. L., Wittenberg, B. A., and Wittenberg, J. B. (1999) *J. Biol. Chem. 274*, 4207−4212.
30. Dou, Y., Admiraal, S. J., Ikeda-Saito, M., Krzywda, S., Wilkinson, A. J., Li, T., Olson, J. S., Prince, R. C., Pickering, I. J., and George, G. N. (1995) *J. Biol. Chem. 270*, 15993−16001.
31. Duff, S. M. G., Wittenberg, J. B., and Hill, R. D. (1997) *J. Biol. Chem. 272*, 16746−16752.
32. Yu, N.-T., and Kerr, E. A. (1988) in *Biological Application of Raman Spectroscopy* (Spiro, T. G., Ed.) pp 39−95, Wiley & Sons, New York.
33. Monti, D., Vodopivec, B., Basilico, M., Olliaro, P., and Taramelli, D. (1999) *Biochemistry 38*, 8858−8863.
34. Stone, J. R., and Marletta, M. A. (1994) *Biochemistry 33*, 5636−5640.
35. Tsubaki, M., Srivastava, R. B., and Yu, N.-T. (1982) *Biochemistry 21*, 1132−1140.
36. Rimai, L., Salmeen, I., and Petering, D. H. (1975) *Biochemistry 14*, 378−382.
37. Deinum, G., Stone, J. R., Babcock, G. T., and Marletta, M. A. (1996) *Biochemistry 35*, 1540−1547.
38. Taylor, C. P. S. (1977) *Biochim. Biophys. Acta 491*, 137−149.

BI991665K